Chemical Engineering Journal 480 (2024) 147934

Contents lists available at ScienceDirect

Chemical Engineering Journal

journal homepage: www.elsevier.com/locate/cej

Direct air capture of CO_2 using green amino acid salts

Arash Momeni [a], Rebecca V. McQuillan [a], Masood S. Alivand [a,b], Ali Zavabeti [a], Geoffrey W. Stevens [a], Kathryn A. Mumford [a,*]

[a] Department of Chemical Engineering, The University of Melbourne, Parkville, Victoria 3010, Australia
[b] Department of Chemical Engineering, Monash University, Victoria 3800, Australia

ARTICLE INFO

Keywords:
Direct air capture
Amino acid salts
Vacuum low-temperature regeneration
Hollow fiber membrane

ABSTRACT

Direct air capture (DAC) of CO_2 using liquid sorbent technology is gaining attention as a promising approach in tackling the looming climate crisis. Despite technical advancements, critical aspects such as contactor selection, energy efficiency, sustainability, and environmental compatibility still pose uncertainties. In this study, various green amino acid salts performances in a DAC system were explored using non-porous hollow fiber membrane contactors (HFMCs). Two DAC absorption and desorption apparatuses were developed. For the DAC-absorption unit, the thermodynamic and kinetic behavior of five types of aqueous amino acid salt solutions were evaluated in long-term operations. High absorption stability for most of the solutions in different solvent loadings (up to 80% CO_2 solvent loaded) were observed and potassium glycinate (GlyK) was selected as the most suitable candidate for DAC. To enhance the CO_2 separation efficiency, parametric analysis on air and solvent flow rates, solvent temperature and concentration were conducted using GlyK. Vacuum low-temperature desorption experiments were carried out with GlyK to evaluate the CO_2 removal efficiency over a range of solvent temperatures and concentrations, CO_2 loadings, vacuum pressures, and vacuum/sweep gas mode. The results successfully quantified the effect of each operational parameter under various conditions on CO_2 removal in a DAC system. Finally, to investigate the impact of membrane characteristics on DAC absorption–desorption performance, a developed and validated model was used. Taken all together, hybrid technology of membrane modules and green amino acid salts is shown to be a viable pathway towards a sustainable DAC process.

1. Introduction

The adverse implications arising from the escalating global emissions of carbon dioxide (CO_2) have evolved into a major point of concern [1]. For the first time in recorded human history, the atmospheric CO_2 concentration has exceeded 420 parts per million, marking a momentous rise of nearly 50 % since the onset of the Industrial Revolution (280 ppm) [2]. As a consequence of this significant rise, the average atmospheric temperature has experienced an approximate 1 °C increase. The primary objective of the Paris Agreement is to set a target of limiting global warming to 2 °C, with a more ambitious goal of possibly reaching 1.5 °C by the end of the 21st century [3]. To accomplish this objective, in addition to significantly reducing human-caused greenhouse gas (GHG) emissions, it is imperative to take sustainable measures for actively removing carbon dioxide (CO_2) through the implementation of Negative Emissions Technologies (NETs) [4]. Among the NETs, CO_2 direct air capture (DAC) has gained growing attention as a viable approach for mitigating climate change popularized by Lackner in 1999 [5]. The viability of DAC operation can be attributed to high capacity, adaptable placement options, and the production of high-purity CO_2 streams. In this approach, ultra diluted CO_2 concentration (~415 ppm) in the atmosphere can be directly captured. Two approaches are considered most promising, adsorption, or absorption [6,7]. Currently, most studies are focused on solid sorbents (Global Thermostat and Climeworks [8]) while limited research and development is occurring in the domain of chemical absorption using well-known liquid sorbents in this field e.g., amine-based solvents. Furthermore, amine-based solvent absorption is undoubtedly one of the most reliable operations of CO_2 mitigation processes and has been used in a large fraction of industrial applications [9,10]. Hence, by prioritizing research and development efforts in this area, valuable knowledge acquired from these successfully implemented large-scale plants can be effectively utilized in the specification of DAC technologies, facilitating its smooth transfer and application. Among the different types of amine-based solvents, amino acid salts are known to be

* Corresponding author.
E-mail address: mumfordk@unimelb.edu.au (K.A. Mumford).

https://doi.org/10.1016/j.cej.2023.147934
Received 11 September 2023; Received in revised form 14 November 2023; Accepted 4 December 2023
Available online 9 December 2023

a promising selection for DAC operation, owing to their unique physical and chemical features such as fast reaction rate, low volatility, low toxicity, and strong resistance to oxygen degradation [11,12]. Nevertheless, since the adoption of liquid sorbents in DAC is an emerging technology, there are number of challenges that need to be addressed to achieve widespread utilization at large scale. One of the main obstacles is the requirement of introducing large amounts of air into the system due to the low concentration of CO_2 in ambient air, which leads to low ratios of solvent to air flow rates [13]. Additionally, typical regeneration processes require high operating temperatures near, 120–140 °C, which leads to high energy consumption (sensible heat plus latent heat). Consequently, these circumstances result in elevated operating costs and, more importantly, thermal degradation of the solvent (e.g., including amino acid salts which are suitable for DAC) [14,15]. Thus, prioritizing further research and development efforts in applying new technologies to address these challenges in DAC operation is of utmost importance.

Hollow fiber membrane contactors (HFMC) are a hybrid technology that benefits from the advantages of both solvent technology and membrane separation [16,17]. Their modular and compact design, flexibility in operation (different L/G ratios) due to a distinct and stable phase interface, large contact area and convenient scalability have made it a viable choice for DAC processes [18,19]. Additionally, by applying vacuum stripping, the operating temperature can be lowered below the solvent boiling point (<100 °C) which will considerably reduce the thermal degradation of aqueous solvents and facilitate use of solar energy for solvent regeneration [20,21]. Also, it will eliminate the necessity for steam in the process and the heating media can be altered to sustainable solar energy. There are vast quantities of work that analyze the absorption–desorption performance of aqueous solvents in different types of HFMCs [22–24]. However, to the best of the author's knowledge, few studies have focused on the application of this system in DAC-absorption processes, and none have investigated it for DAC-desorption.

Here, for the first time, the experimental and theoretical analysis of green amino acid salt sorbents in low temperature regeneration DAC operation are evaluated. Two DAC apparatuses, absorption and desorption, are designed and developed using commercial HFMCs, made of non-porous hydrophobic polydimethylsiloxane (PDMS). In the DAC-absorption section, the kinetics and equilibrium performance of five amino acid salts, potassium glycinate (GlyK), potassium lysinate (LysK), potassium sarcosinate (SarK), potassium prolinate (ProK), and potassium histidine (HisK) were examined in long-term operation (zero CO_2 solvent loading to completely saturated at DAC conditions). As GlyK was found to be the most viable option for DAC operation, further long-term trials on important process parameters e.g., solvent temperature and concentration for the GlyK were conducted. For the low temperature DAC-desorption section, the kinetic performance analysis for the GlyK was accomplished at different solvent loadings for various operational conditions (solvent temperature and concentration, vacuum pressure, sweep gas effect). Finally, a validated DAC model with acquired absorption and desorption bench-scale data in Aspen Custom Modeler (ACM) was used to study the impact of membrane module characteristics on CO_2 separation efficiency. The findings of this study give deep insight into the operability and CO_2 absorption–desorption performance of green amino acid salt sorbents in a DAC operation, which is the start of a new path towards sustainable, cost-effective DAC.

2. Materials and methods

2.1. HFMC

A commercial non-porous PDMS HFMC (Permselect-MedArray, Ann Arbor, Michigan, USA) was selected and utilized. The non-porous (dense) hydrophobic PDMS has a high level of resistance to pore wetting, a critical factor when applying HFMCs, especially under high temperature operation. This guarantees a flexible and stable operation in the long-term, as well as minimizes solvent loss [22]. Moreover, the PDMS exhibits suitable thermal and chemical stability which is important when considering long-term operation [25]. The module consists of 30,000 fibers that offer a contact area of 2.1 m^2 and is operated in a counter-current parallel flow configuration. Table 1 lists the details of the membrane modules used.

2.2. Material

Glycine, L-lysine hydrochloride, sarcosine, L-proline, and histidine were selected and purchased from Sigma Aldrich for the screening experiment. The amino acid salts had a purity greater than 98.0 % and were used without purification. Potassium hydroxide with a purity of more than 85.0 % was purchased from Chem-Supply, Australia. A nitrogen gas cylinder (N_2, 99.9 %) was purchased from BOC Gases Company, Australia.

2.3. Experimental design

The chemical structures of the amino acid salts used are depicted in Fig. 1a. GlyK, SarK, ProK, HisK solutions were prepared by adding deionized water with an equimolar amount of KOH. For LysK solution preparation, L-lysine hydrochloride was mixed with double molar equivalents of KOH in deionized water to neutralize HCl in the lysine structure. Furthermore, the prepared solutions were utilized in the developed DAC units (Fig. S1) to analyze absorption–desorption behaviour.

2.3.1. Absorption apparatus

The schematic of the experimental DAC-absorption setup using HFMC is illustrated in Fig. 1a. More detail can be found in Fig. S1a. An in-house compressed dry air line in the laboratory was used to supply the required amount of air into the lumen side of the HFMC with an average specification of ~ 415 ppm and a relative humidity (RH) of ~ 3 % (at ambient temperature). To adjust the air pressure, a regulator (Swagelok) was installed on the air line. A gas flow controller (GFC) from Aalborg (0–100 L/min) was utilized to regulate the air volume flow rate. Once the desired value was set on the GFC, air was introduced into the module. Two online CO_2 analyzers (CO_2Meter, 0–1 %, with an accuracy of ± 30 ppm) and two online temperature/RH sensors (HOBO, 1–100 %) were installed at the inlet and outlet air streams to monitor and log the CO_2 content and temperature/RH during operation, respectively. In order to monitor the air pressure drop along the membrane module, two pressure gauges (Braeco, 0–100 kPa) were located at the inlet and outlet of the module. After achieving a stable airflow and measurement values, 500 ml of the prepared amino acid salt solution was transferred into a bottle and circulated in a closed loop on the shell side of the module via a peristaltic pump (Master Flex, Easy Load II). Sample points were considered at the inlet and outlet of the membrane module to measure the solvent loading using the Chittick Apparatus (Fig. S2). During operation, the solvent and the air were routed to the module in the counter-current mode, and the transfer of CO_2 and subsequent increase in solvent loading occurred over time. The experiment ended when the

Table 1
Specification of the applied HFMC.

Supplier	PermSelect
Membrane Material	PDMS (Silicone)
Module Diameter	8.9 cm
Module Length	14.2 cm
Fiber ID	190 μm
Fiber OD	300 μm
Fiber Wall Thickness	55 μm
Effective Fiber Length	7.4 cm
Number of Fibers	30,000
Membrane Area (based on fiber OD)	2.1 m^2

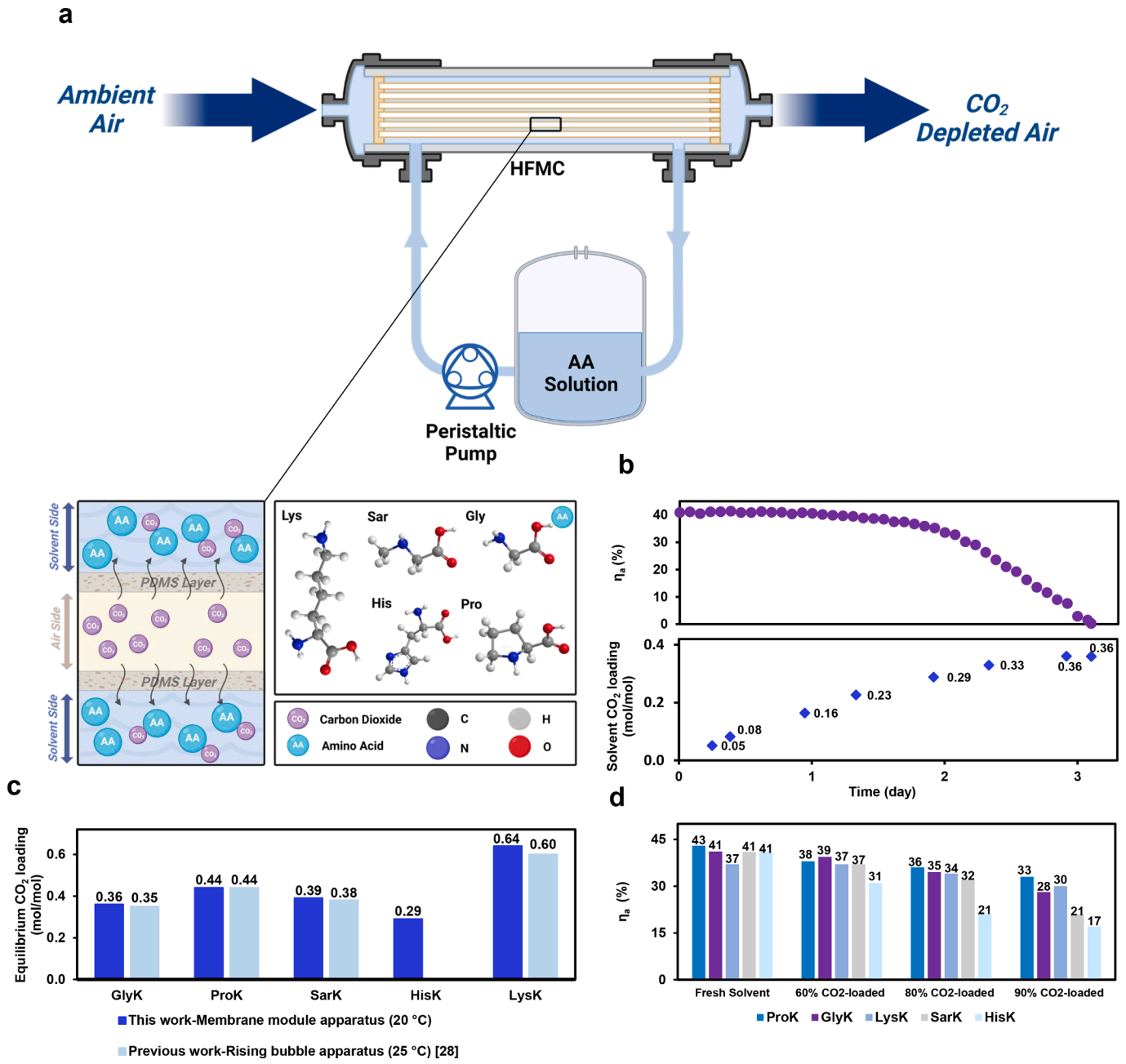

Fig. 1. a) Schematic diagram of DAC-absorption using HFMC, absorption mechanism, and amino acid salts structures **b)** Absorption efficiency (η_a) of 1 M GlyK in a long-term operation at different solvent loadings. **c)** The DAC-equilibrium CO_2 loading points for different amino acid salt solutions and the comparison with previously obtained DAC-equilibrium data [28]. **d)** Absorption efficiency (η_a) of 1 M of different amino acid salt solutions at various solvent loadings. All data were obtained at 20 °C, air flow rate = 7.2 L/min, and solvent flow rate = 0.25 L/min.

concentration of CO_2 in the outlet reached within ± 10 ppm of the inlet CO_2 concentration. This criterion signifies that the solvent had reached equilibrium and no longer possesses further considerable absorption capacity. The temperature of the solvent was maintained at the desired value using a water bath circulator (JULABO) while a thermocouple data logger was inserted into the solvent bottle to accurately track temperature during experiments. It is noted that to keep the temperature of the solvent constant, and minimize heat transfer to/from the surroundings, the membrane module and associated lines and valves were insulated.

To analyze the CO_2 separation efficiency, equations (1) and (2) were employed.

$$\eta_a = \frac{Q_{in}C_{in} - Q_{out}C_{out}}{Q_{in}C_{in}} \times 100 \quad (1)$$

$$J_a = \frac{Q_{in}C_{in} - Q_{out}C_{out}}{A} \quad (2)$$

where η_a is the CO_2 absorption efficiency (%), J_a is the CO_2 absorption flux (mol/m^2·s), C_{in} and C_{out} are the CO_2 concentrations for the inlet an outlet air (mol/m^3), Q_{in} and Q_{out} are the inlet and outlet air flow rates (m^3/s), and A is the membrane contact area (m^2).

2.3.2. *Desorption apparatus*

As depicted in Fig. S1a, the membrane vacuum regeneration technology entails two distinct sides: the solvent side and the vacuum/sweep

gas side. 500 ml of DAC CO_2-loaded amino acid salt solution (from the DAC-absorption unit) was put into a bottle and circulated on the lumen side via a pump (Master Flex, Easy Load II). Prior to entering the module, the solvent passed through a coil immersed in an oil bath (JULABO) to be heated to the desired temperature. Due to the elevated operating temperature (70–90 °C), the apparatus was insulated using glass wool. The solvent temperature and pressure were monitored by a thermometer (OMEGA) at the inlet and two pressure gauges (Braeco, 0–100 kPa) at the inlet and outlet of the membrane module, respectively. Additionally, sample points were provided to measure the CO_2 content using the Chittick apparatus (Fig. S2). When the solvent temperature reached the predetermined set value, it was regarded as the start point of the experiment. At this stage, the first solvent sample was extracted from the system, and a vacuum pressure/sweep gas was applied (Laboratory vacuum pump) on the shell side. To investigate the desorption efficiency at different solvent loadings, operation was conducted for 90 min, during which, a sample was extracted to measure the CO_2 content at every 15 min for the first 60 min. The CO_2 removal efficiency and flux were then calculated based on the obtained loading values and solvent CO_2 content according to equations (3) and (4). After the final sample was collected at the 90-minute mark, operation was considered complete. Two vacuum pressure gauges (Braeco, −100 kPa to 0) were placed at each end of the module to monitor the pressure level throughout the operation. To condense the transferred water across the fibers and recycle it back to the solvent container, an acetone-ice bath trap (-15 ± 5 °C) was installed in-line at the outlet.

For sweep gas experiments, N_2 was used as a sweep gas and introduced to the shell side under vacuum condition. To monitor the volume flow rate of N_2, a rotameter was utilized.

$$\eta_d = \frac{\alpha_i - \alpha_j}{\alpha_i} \times 100 \tag{3}$$

$$J_d = \frac{C_i - C_j}{A\Delta t} \tag{4}$$

η_d is the CO_2 desorption efficiency (%), J_d is the CO_2 desorption flux (mol/m^2·s), C_i and C_j are the CO_2 mole content at time i and j, α_i and α_j are the solvent loading values at time i and j (mol/mol), and A is the membrane contact area (m^2) and Δt is the time difference between i and j (s).

3. Results and discussion

3.1. DAC-absorption

To better understand and optimize the performance of the developed system, an initial parametric analysis was completed to assess the appropriate air and liquid flow rates. To do this, fresh GlyK was used due to its desirable properties and similar CO_2 absorption performance to monoethanolamine (MEA), a benchmark sorbent for chemical absorption in CO_2 capture [26]. According to Fig. S3, increasing the air flow from 7.2 L/min to 17.3 L/min, decreases the absorption efficiency by a considerable amount, ~58.5 %. This can be attributed to several factors. As the air flow rate increases, two phenomena occur simultaneously with counteracting effects. The first one is the enhancement of the mass transfer coefficient on the air side due to increased turbulence. The second one is the decrease in retention time, which limit the mass transfer between the air and solvent phases, resulting in lower overall efficiency. The significant drop in overall efficiency indicates the dominance of the latter factor which can be related to the type of membrane and the distribution of resistances within the module. Hence, the 7.2 L/min air flow rate, which exhibits maximum efficiency and introduces an acceptable number of CO_2 moles to the system, was selected for use in all additional experiments.

In the next step, the variation of the solvent flow rate was also assessed. Flow rates were operated between 0.1 and 0.5 L/min and did not display a noticeable impact on the system behavior (data not shown). Within the investigated temperature range (10–30 °C), there was minimal change in the observed CO_2 flux and overall efficiency, further confirming that the membrane is the main contributor to mass transfer resistance [27].

3.1.1. Screening amino acid salt sorbents

As shown in Fig. 1a, five amino acid salts with different structures (short chain and long chain) were selected and prepared to a concentration of 1 M to be tested in the DAC-absorption unit. In order to examine the DAC equilibrium points and the CO_2 absorption kinetics at different solvent loadings, the DAC-absorption apparatus was continuously operated for several days until solvent saturation was reached. Fig. 1c shows the resulting DAC equilibrium points of the varying amino acid salts acquired at 20 °C. The collected data was compared with the data obtained at 25 °C from the rising-bubble setup in our recent study [28]. The strong agreement between these datasets provides compelling evidence for the reliability and precision of the data obtained through membrane technology, which holds the potential for large-scale utilization. According to Fig. 1c, LysK has the highest DAC CO_2 loading capacity of 0.64 mol/mol (mol CO_2/mol solvent), attributed to its long-chain structure containing two amino groups that enable enhanced CO_2 absorption capacity. Among the short-chain solvents, ProK, SarK, GlyK, and HisK exhibit smaller values of 0.44, 0.39, 0.36, and 0.29 mol/mol, respectively. HisK demonstrated the lowest value of 0.29 despite having more amine functional groups in its structure compared to other short-chain amino acid salts. This could be attributed to the observed precipitation during operation, and the behavior and reaction of the specific amine groups to extremely low concentrations of CO_2 in the atmosphere.

By comparing the difference between the amount of CO_2 in the inlet and outlet air, as well as measuring the solvent CO_2 loading at regular intervals, a consistent evaluation of the CO_2 DAC-absorption performance at various solvent loadings was accomplished. Fig. 1b shows the GlyK absorption performance at different solvent loadings at 20 °C. At experiment commencement, when the solvent was fresh, the absorption efficiency was 41 %. A minimal loss (~6%) in CO_2 uptake was observed throughout a substantial portion of the operating period up to a solvent loading of 0.29 mol/mol (80 % CO_2 loaded solution). This is related to the non-porous characteristics of the membrane, which prevents pore-wetting and solvent entrainment, two major issues that hinder stable operation. This is also related to the shape of the vapor liquid equilibria (VLE) curves of 1 M GlyK [29]. A decline in absorption performance occurred when the solvent loading reached 0.29 mol/mol, caused by the solvent approaching its equilibrium point. This trial with GlyK was repeated three times to assess the repeatability of the DAC-absorption rig (Fig. S4), a factor which was found to be compelling.

Long-term analyses were also conducted for LysK, ProK, SarK, and HisK at 20 °C (Fig. S5). Fig. 1d illustrates the CO_2 absorption efficiency data for all five amino acid salts at various levels of loading, extracted from Fig. S5. Among the fresh solvents, ProK showed the highest CO_2 uptake rate with 43 %, and in contrast, LysK was the lowest with 37 %. GlyK, SarK, and HisK exhibited the same efficiency value of 41 %. This similarity can be related to ultra-low CO_2 concentration in air and also the resistance of the thick (55 μm) non-porous PDMS layer of membrane which governs the CO_2 mass transfer. Until reaching 80 % solvent loading, all amino acid salts except HisK demonstrated stable CO_2 uptake with minimal losses ranging from 6 to 9 percent, which can be explained by the VLE curves of the amino acid salts [29] and hydrophobic characteristics of the dense membrane layer. HisK, on the other hand, exhibited a dramatic loss in performance in CO_2 capture, likely due to the observed precipitation during operation. Importantly, it is observed that ProK, LysK, and GlyK maintained an efficiency of around 30 % in absorbing CO_2 even up to a 90 % CO_2 loading level. This highlights the capability of the hybrid technology of amino acid salts and HFMCs to utilize the maximum capacity of the solvent in DAC-absorption. Hence, ProK, LysK, and GlyK were chosen as the desired

amino acid salt solutions for DAC-absorption due to their favorable kinetic performance under different solvent loading conditions.

Another important factor to consider when selecting an appropriate solvent is the cyclic capacity, which determines the sorbent's ability to effectively capture and release CO_2 during absorption–desorption cycles in a continuous process. Based on our recent study [28], the cyclic capacity of ProK, LysK, and GlyK in DAC operation was recorded at various temperature ranges (25–70 °C, 25–85 °C, and 25–98 °C); LysK and GlyK stood out as the top sorbent in terms of cyclic capacity across all temperature ranges. Hence, the selection was narrowed down to these solvents. Upon comparing these two, GlyK was chosen for further analysis due to its superior desorption kinetics [28], easier preparation as aqueous solvent, and its acceptable cyclic capacity range. It is worth mentioning that LysK exhibited challenges in dissolving within water for aqueous solvent preparation for higher molarities, notably at a concentration of 3 M (Fig. S6). This issue can be related to the long-chain structure and high molecular weight of L-lysine, which lowers its solubility and poses challenges in achieving dissolution at higher concentrations.

3.1.2. Solvent temperature

To gain insight into how temperature affects equilibrium and the kinetics of CO_2 absorption at different loading levels, the DAC-absorption rig was run continuously with GlyK over several days at three distinct temperatures (10, 20, 30 °C). Fig. 2a depicts the equilibrium points obtained at three different temperature levels. As the temperature rises, the solubility of CO_2 in the solvent decreases, resulting in lower equilibrium solvent capacity. Another important factor is the water transfer through the membrane at different temperatures. Since the system has a relatively low RH feed air, the transfer of water from the liquid side to the air side was expected. In Fig. 2a, average values of the RH in the air outlet during operation at the three different temperatures are presented. As the temperature increased, the water partial pressure on the liquid side increased, reinforcing the transfer of water across the membrane and leading to higher recorded values of RH outlet. The rise in temperature from 10 °C to 30 °C resulted in an increase in the average RH at the outlet from 40 % to a nearly saturated state (150 % increase), thereby emphasizing the impact of the solvent temperature.

Fig. 2c displays the CO_2 absorption flux at three different temperatures under various solvent loading conditions. Upon comparing the data for 10 °C and 20 °C, no major change was observed which can be attributed to the dominance of the dense layer of the membrane acting as the primary resistance for CO_2 transfer. At higher loading levels, the flux at 10 °C outperformed the flux at 20 °C, related to the higher saturation point of GlyK at 10 °C (Fig. 2c). Interestingly, when operating at 30 °C, a major reduction in performance was recorded across all solvent loading values. Typically, one would expect an increase in the mass transfer coefficient and flux with an increase in temperature due to the accelerated reaction rate in the solvent boundary layer and a decrease in solution viscosity. However, in this case, since the membrane phase dominates the mass transfer, and also there is a decrease in absorptive capacity, the enhanced effects resulting from increased temperature were not observed. Therefore, based on the results, 20 °C is deemed optimal for DAC-absorption using a non-porous membrane module, as it provides acceptable solvent capacity, kinetic performance, and energy demand input.

3.1.3. Solvent concentration

To examine the impact of solvent concentration on CO_2 uptake capacity, kinetics, and any potential precipitation and operational issues across various solvent loadings, two sets of long-term trials were conducted using 2 M and 3 M GlyK. Fig. S7 depicts the CO_2 absorption flux for GlyK 1 M, 2 M, and 3 M versus solvent CO_2-loading. As it is shown, no major change was achieved by increasing the solvent concentration at different levels of solvent loading. This behavior can be related to several factors, including the simultaneous two-fold effect, one being decreased CO_2 diffusivity in solvent (due to increased solvent viscosity) and the other being an increased mass transfer coefficient. Also, the presence of a dense PDMS layer, and the ultra-low concentration of CO_2 in the air can reduce the impact of solvent concentration. On the other hand, according to Fig. 2b, the CO_2 uptake capacity (CO_2 mol/solvent liter) for 2 M and 3 M substantially increased (doubled and tripled) as a

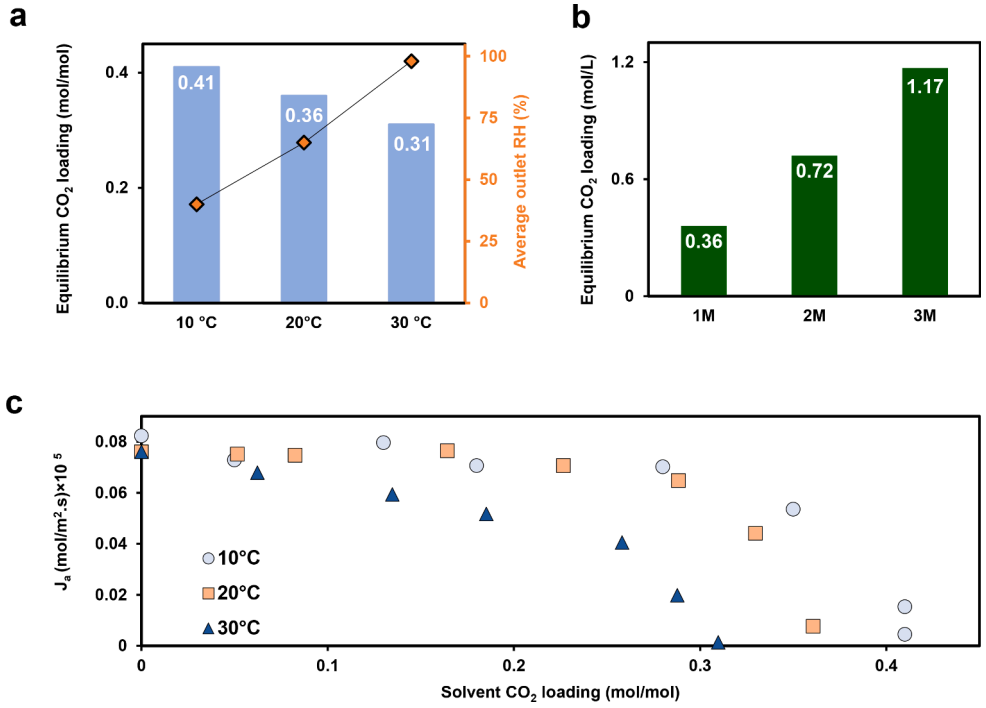

Fig. 2. a) The DAC-equilibrium point and average outlet RH% for 1 M GlyK at different temperatures. **b)** The DAC-equilibrium point for different GlyK concentrations at 20 °C. **c)** The CO_2 absorption flux (J_a) of 1 M GlyK at different temperatures in various solvent loading conditions. All data were obtained at air flow rate = 7.2 L/min, and solvent flow rate = 0.25 L/min.

result of the increased molarity. Since no operational problems or precipitation were observed throughout the operations and with similar kinetic performance, selecting a higher level of solvent concentration in DAC-absorption is advantageous due to a higher absorption capacity. This implies reduced use of solvent (at least halved) in the absorption–desorption cycles is possible, leading to lowering the size of the heating equipment and the associated energy requirements.

3.2. Low-temperature DAC regeneration

Due to the imperative role of low-temperature regeneration in DAC processes, regarding the capacity of the unit, thermal degradation of the solvent, and a major part of operating cost, a comprehensive study with various effective factors was completed to optimize the efficiency of the CO_2 stripping process.

As discussed in the absorption section, among the screened amino acid salt aqueous solutions, GlyK was chosen as it possesses favorable

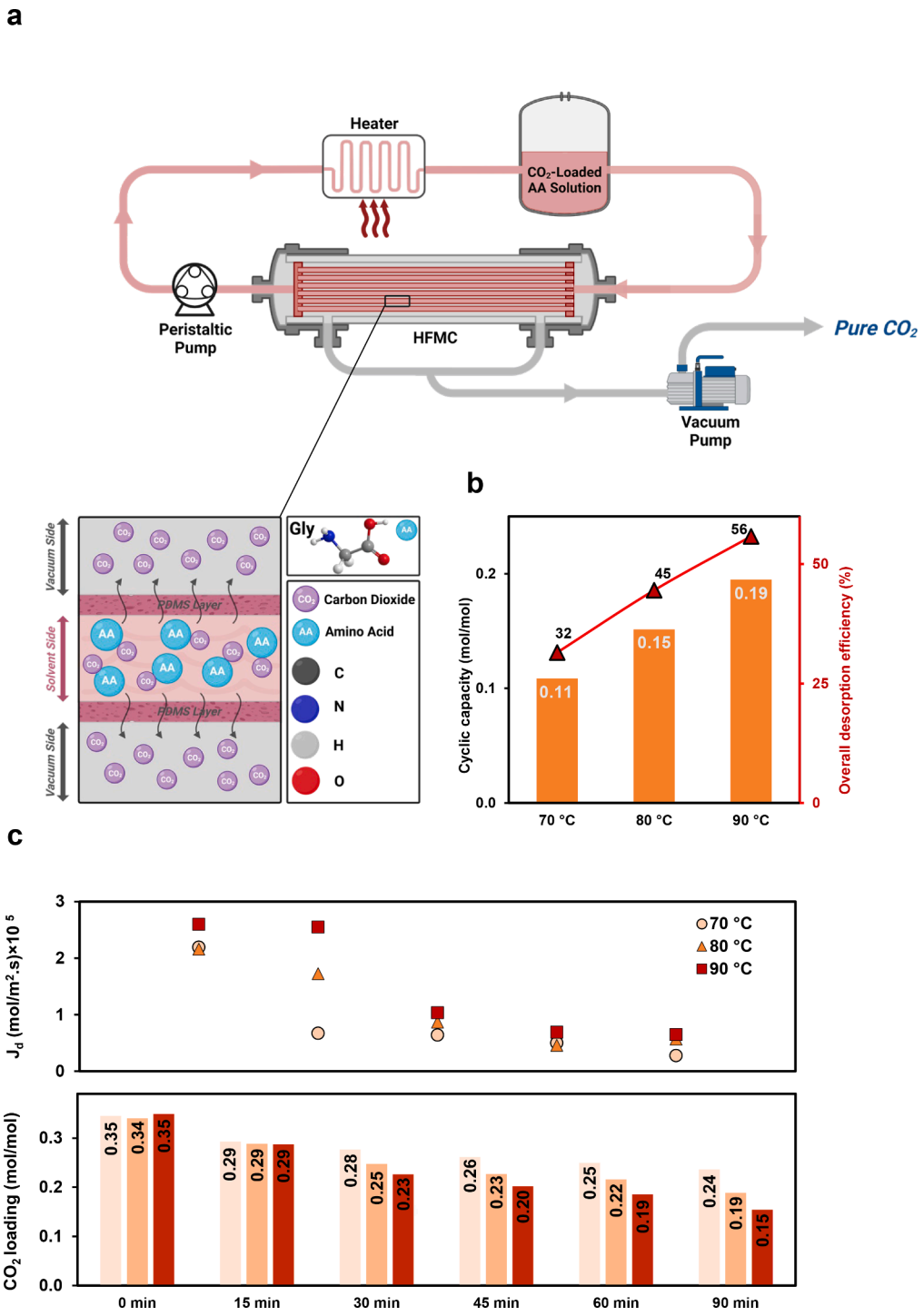

Fig. 3. a) Schematic diagram of low-temperature DAC regeneration using HFMC, desorption mechanism, and Gly structure **b)** 1 M GlyK cyclic capacity and overall desorption efficiency at different regeneration temperatures. **c)** 1 M GlyK DAC-desorption flux (J_d) at different temperatures and solvent CO_2 loadings. All data were obtained at 21 $kPa_{(a)}$, and solvent flow rate = 0.25 L/min.

properties such as absorption kinetics, cyclic capacity, being less challenging in terms of operational problems and solution preparation for high molarities, and having a high desorption kinetics [28]. Thus, the low temperature regeneration trials were conducted with an aqueous solution of the GlyK. All the stripping tests were accomplished under vacuum conditions (21–81 $kPa_{(a)}$) without sweep gas, with the exception of one trial used to investigate the effect of the sweep gas on performance (section 3.2.4). The solvent flow rate was maintained at 0.25 L/min, equal to the absorption section. Each operation continued for 90 min to be able to observe the effect of solvent loading on CO_2 removal efficiency.

3.2.1. Solvent temperature

Membrane contactor tests were performed within a temperature range of 70 to 90 °C under a vacuum pressure of 21 $kPa_{(a)}$, with the results presented in Fig. 3. The schematic of the experimental DAC-desorption setup using HFMC is shown in Fig. 3a. At the beginning of each trial, before applying vacuum pressure and as the solvent was preheated to the desired temperature, a sample were taken out of the system to measure the preheating effect on CO_2 removal (Fig. S8a). All the DAC CO_2-loaded GlyK solutions started with a similar level of CO_2 content, approximately 0.34–0.35 mol/mol. To assess the repeatability and accuracy of the DAC-desorption apparatus, three consecutive trials were carried out at 70 °C, and the results are plotted in Fig. S8, along with the temperature profile which showed good consistency. Fig. 3b highlights the cyclic capacity of GlyK at various temperatures. Notably, as the temperature increased from 70 °C to 90 °C, there was an increase of over 75 % in cyclic capacity and overall desorption efficiency. This indicates that each 10 °C can add 0.04 mol CO_2 per mol of solvent to the capacity of the system. Thus, increasing the temperature directly and positively impacts the stripping performance.

In Fig. 3c, the desorption kinetics at different temperatures and solvent loadings are depicted. Comparing the CO_2 DAC-desorption flux with the acquired ones for DAC-absorption, the values are significantly higher because of the higher operating temperature, increased CO_2 driving force across the membrane and faster CO_2 diffusivity. Between 0.35 and 0.29 mol/mol (~80 % CO_2-loaded), the highest kinetic rates were observed for all the temperature levels. This can be related to the higher CO_2 content in the solvent at the beginning of the test, which increased the CO_2 driving force across the membrane. For loadings lower than 0.29 mol/mol, dramatic kinetic losses occurred at 70 °C. In this range, since the CO_2 desorption flux for 90 °C remained constant with the highest value, it suggests that the drop in the desorption performance for 70 °C and 80 °C is attributed to the thermodynamics of the solution and not a membrane-related issue (swelling or pore-wetting). In fact, working at higher temperatures led to higher equilibrium partial pressures of CO_2, chemical reaction equilibrium constants, diffusion coefficients, and reaction kinetics [29]. For 80 °C and 90 °C, as the solvent loading fell below 0.25 and 0.23 mol/mol (65–70 % CO_2-loaded), the average CO_2 flux declined and remained close to the kinetic values obtained for 70 °C, which highlights the effect of CO_2-loading on stripping efficiency. Therefore, to be able to maintain the kinetic performance within a suitable range for a major part of the stripping operation, working above 0.23 mol/mol for 1 M GlyK is advantageous (~65 % CO_2-loaded). In addition, this level of CO_2-loaded solvent allows for maximum and stable absorption performance in the DAC-absorption section (Fig. 1b,d). It is worth mentioning that raising the temperature to a higher value of 90 °C allows for further reduction of the lean loading value and enhances stripping performance. However, due to the limitations of the apparatus, temperatures higher than 90 °C were not investigated. Considering the acceptable cyclic capacity, desorption efficiency, and the avoidance of potential operational issues, further experiments were conducted at 80 °C.

3.2.2. Vacuum pressure

Experiments were conducted at 80 °C under various vacuum pressures, 21–81 $kPa_{(a)}$, applied to the shell side of HFMC, and the impact on desorption efficiency was assessed. Interestingly, according to Fig. 4a, a pronounced improvement was observed with a 60 kPa change in vacuum pressure, resulting in a 221 % enhancement in overall desorption efficiency. The favorable effect of the vacuum is explained by the decreased CO_2 partial pressure on the shell side, which increased the mass transfer driving force for CO_2 desorption. Additionally, the reduced pressure on the permeate side of the membrane endured at higher vacuum levels, enhanced the driving force for CO_2 desorption.

Fig. 4b, presents the desorption kinetics at three levels of vacuum pressure, 21, 51, and 81 $kPa_{(a)}$. In the initial stages of the process, where the solvent's CO_2 content is at its maximum, the CO_2 flux for 21 $kPa_{(a)}$ was over 1.4 times higher than for 51 and 81 $kPa_{(a)}$. However, as the operation continued and the solvent became leaner (~0.23 mol/mol), the CO_2 removal performance of the low vacuum pressure reduced and became similar to the other vacuum levels. This is attributed to a reduction in the CO_2 partial pressure, which appears insufficient to activate enhanced CO_2 diffusion for achieving a higher flux. Hence, to effectively maximize and harness the strength of high vacuum pressure during low temperature DAC regeneration, operating above 0.23 mol/mol (~65 % CO_2-loaded) for 1 M GlyK at 80 °C is deemed suitable. Also, it is evident that the vacuum pressure for effective CO_2 removal should be as low as practically possible for non-wetting membranes, taking into account the energy requirements within the limitations of the final application.

3.2.3. Solvent concentration

Here, the influence of GlyK concentration (1, 2, and 3 M) on the CO_2 desorption flux and the capacity of the system were studied. According to Fig. 4d, higher molarities provided higher CO_2 removal flux throughout a major part of operating period (complete data set is provided in Fig. S9). This behavior is linked to the increased quantity of formed carbamate molecules present during DAC-absorption at increased solvent concentrations. As a result, a larger amount of accessible CO_2 will be available for stripping from the solution, leading to an increase in the CO_2 concentration and the corresponding driving force. From a capacity point of view, based on the discussion in Section 3.1.3 (Fig. 2b), by increasing the GlyK concentration, the number of CO_2 moles required to reach equilibrium is increased. In Fig. 4c, the total amount (g) of CO_2 removed for different GlyK concentrations through low-temperature vacuum regeneration is indicated. Comparing 1 M to 2 M and 3 M, a 47 % and 65 % enhancement was recorded. It is notable that the improvement rate between 1 M and 2 M is higher than 2 M to 3 M because of increased solvent viscosity, which leads to slower CO_2 diffusion [30,31]. Therefore, due to the enhanced kinetics and capacity in the DAC-desorption section, and since no precipitation or operational challenges were identified during the trials, utilizing higher molarities for GlyK is recommended.

3.2.4. Sweep gas

To demonstrate and analyze the effect of sweep gas on CO_2 removal efficiency, a combined sweep gas/vacuum mode trial was conducted. 5 L/min of N_2 was introduced to the shell side while applying vacuum pressure (21 $kPa_{(a)}$); the flow rate was monitored continuously using a flow meter during operation. Interestingly, no enhancement in CO_2 stripping performance was recorded in comparison to vacuum alone (Fig. 4f). This is likely related to the membrane dense layer, which controls the CO_2 mass transfer in the membrane module. Generally, introducing a sweep gas to the system reduces the resistance on the vacuum side for CO_2 transfer due to enhanced evaporation and the elimination of a condensed water film layer [32]. However, since the membrane's dense layer is the dominant resistance in CO_2 removal, no improvement in stripping efficiency was observed. On the other hand, a dramatic change in water transfer across the membrane occurred. According to Fig. 4e, in sweep gas/vacuum mode, over three times the amount of water was added for compensation during operation. This is

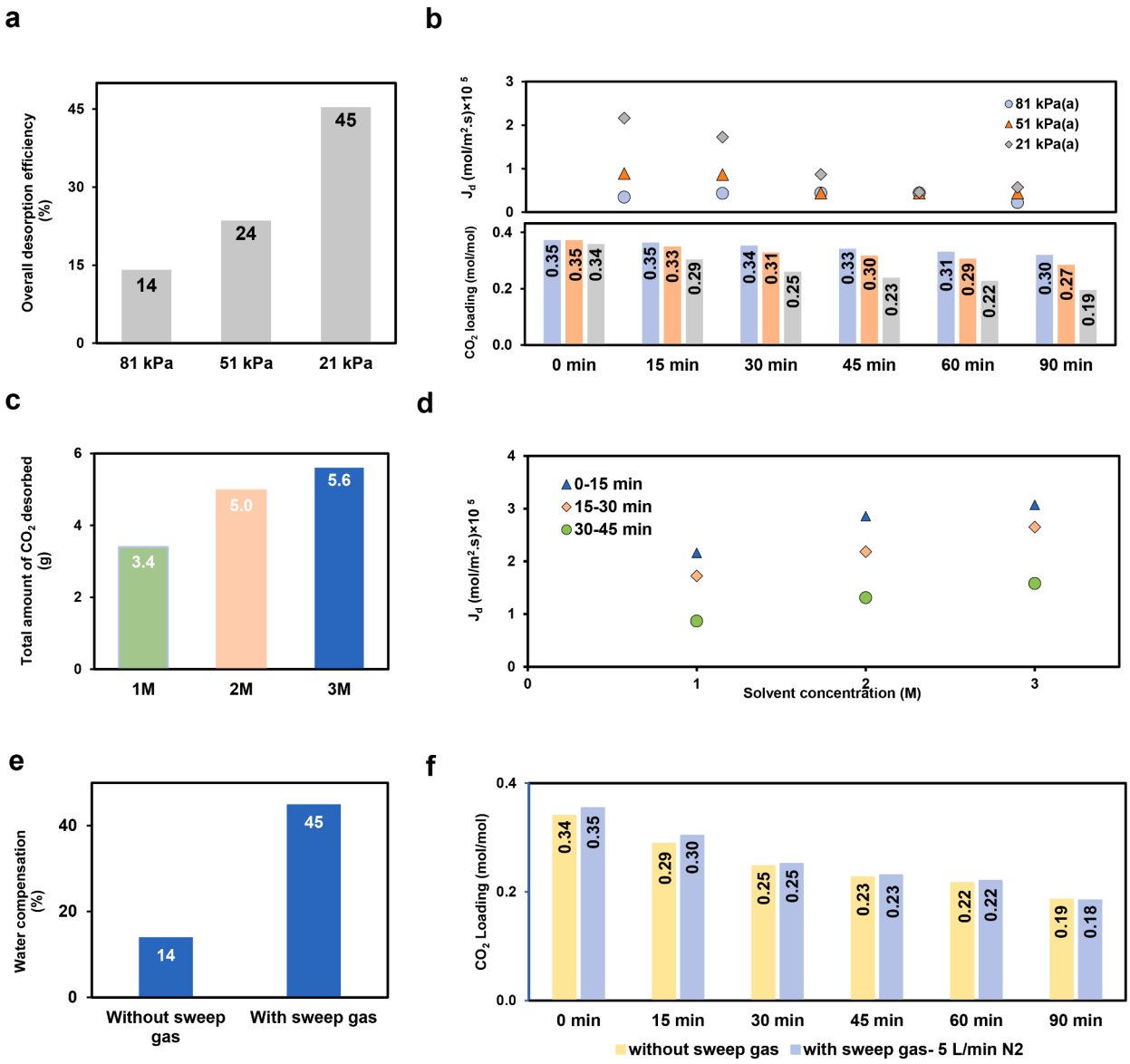

Fig. 4. **a)** 1 M GlyK overall DAC-desorption efficiency at different vacuum pressures. **b)** 1 M GlyK DAC desorption flux (J_d) at different vacuum pressure levels and solvent loadings. **c)** Total g of removed CO_2 using different GlyK concentration at 21 $kPa_{(a)}$. **d)** DAC desorption flux (J_d) of GlyK at different level of concentration at 21 $kPa_{(a)}$. The result of two modes of trials for Vacuum, and Vacuum/sweep gas mode **e)** Water make-up percentage. **f)** CO_2 solvent loading values through time. The data were obtained at 80 °C, and solvent flow rate = 0.25 L/min.

attributed to the elimination of the mentioned condensed water film layer, leading to an increased water flux across the membrane. In addition, applying sweep gas caused less condensation and collection of water in the acetone-ice bath trap (due to the shorter residence time of vacuum side stream in the trap). This implies there will be greater energy demand in the condenser during sweep gas operation.

3.3. Simulation

Apart from the experimental approach detailed in the previous sections, a more detailed analysis of the overall mass transfer coefficient, K, was also required to evaluate the possibilities and limitations of membrane contactors used in the DAC-absorption and desorption processes. Hence, a mathematical model developed in Aspen Custom Modeler (ACM) by McQuillan et al. [29] and validated using the data reported in this work, was used to help characterize and understand the performance of the described HFMC system.

Even though the thick, dense PDMS layer in the membrane (55 μm) provides stable operation without pore-wetting and favorable mechanical stability, it introduces considerable mass transfer resistance. In such cases, one of the most effective mechanisms to enhance the overall mass transfer efficiency is to reduce the membrane thickness. Therefore, the validated model was used to precisely determine the mass transfer resistance contribution of each phase in the gas–liquid membrane module at different thickness levels of the dense PDMS layer and its effect on DAC-absorption performance. According to Fig. 5a, 5b, for the 55 μm thickness membrane, over 80 percent of the total resistance is included in the membrane phase, making the system less responsive to operating conditions. Decreasing the thickness from 55 μm to 25 μm and 10 μm, increased the gas phase contribution to the overall mass transfer, and a steep increase in overall absorption efficiency from 41 % to 73 % was observed. Further reducing the thickness of the dense layer to a minimum value of 1 μm, the gas phase became the governing phase, and the absorption performance rose to more than 80 %. These results highlight the significant influence of the dense layer thickness on the overall membrane module performance. Also, it shows HFMCs can be a

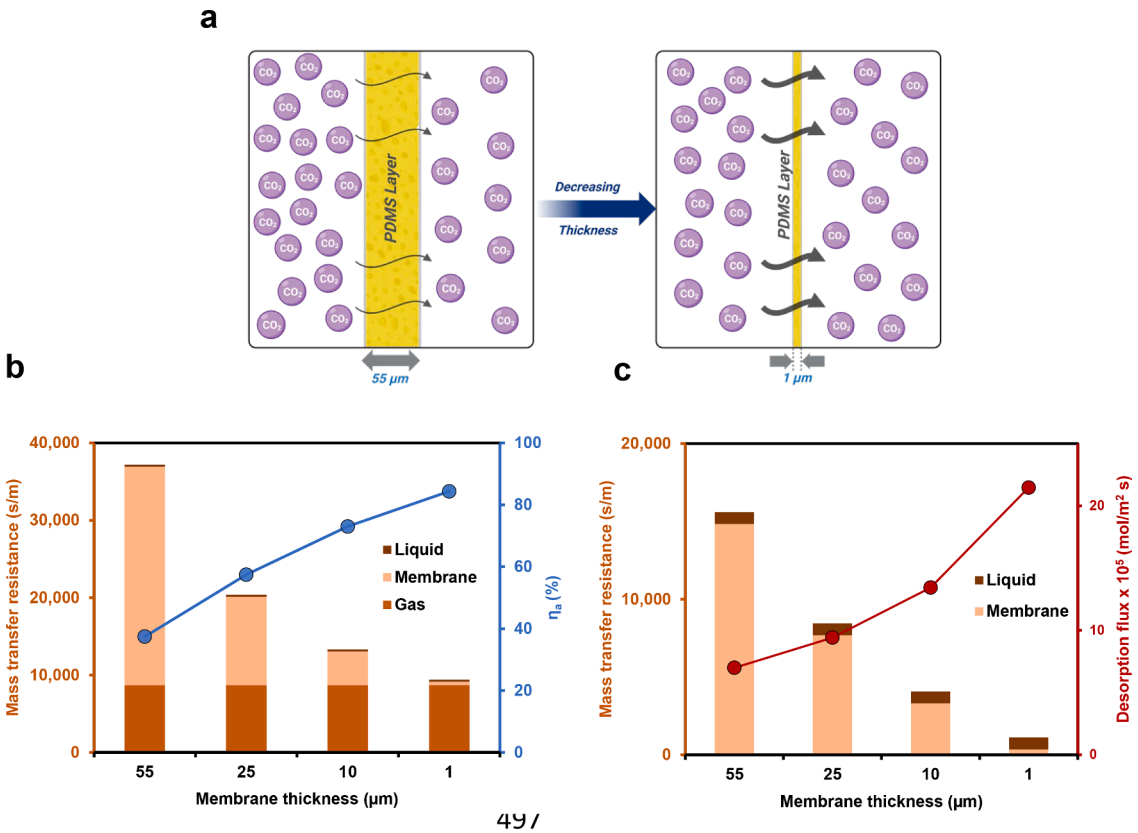

Fig. 5. **a)** Schematic of dense membrane layer thickness effect on the CO_2 separation efficiency. Dense membrane layer thickness effect on **b)** Absorption efficiency **c)** Desorption flux using developed model.

high-efficient and viable technology for large-scale utilization of DAC [29]. Meanwhile, it is noted that more experimental studies are necessary to examine the effect of thin dense layer membranes on the mechanical and thermal stability and pore-wetting phenomena (in porous support) in DAC operation.

To study the effect of membrane module characterization during low-temperature, vacuum regeneration in DAC operation, a series of simulations were conducted at 80 °C for 1 M GlyK to analyze the mass transfer resistance of each phase at different membrane thicknesses, and its impact on stripping performance. As shown in Fig. 5c, the membrane phase accounts for a majority of the CO_2 mass transfer resistance during the regeneration process. As the membrane thickness decreased from 55 to 1 μm, a > 200 % enhancement in CO_2 flux was achieved. In this condition, liquid is indicated as the dominant phase. Nevertheless, it is important to note that DAC stripping operations deal with lower CO_2 content in solvents and CO_2 partial pressures compared to conventional CO_2 stripping units designed with flue gas specifications. This will lead to a lower ratio of CO_2 to water vapor during the high-temperature process, which highlights the importance of the hydrophobic characteristics of the membrane during DAC regeneration. Since vacuum low-temperature regeneration with membrane modules has a high potential for utilization in the DAC processes, further experimental long-term trials are needed on GlyK with a lower membrane thickness to accurately analyze CO_2 and water transfer.

4. Conclusion

This paper presents a successful demonstration of CO_2 separation efficiency in a DAC system through lab-scale experiments and simulations. Trials under various operating conditions, utilizing non-porous HFMCs and different types of environmentally friendly amino acid salt aqueous solutions for absorption and vacuum low-temperature desorption were conducted. Parametric studies were carried out to optimize the CO_2 flux and separation efficiency. Regarding absorption, five amino acid salts were screened in long-term operation at 20 °C. Stable CO_2 absorption performance over a major part of the experiment highlighted the beneficial use of hydrophobic membranes and green amino acid salts. GlyK was selected as the most suitable solvent for DAC in terms of kinetic performance, cyclic capacity, non-precipitating behavior at different levels of concentration and loading, and ease of preparation. Furthermore, it was shown that, DAC-absorption CO_2 flux and capacity is optimized by operating at 20 °C, a suitable solvent temperature when considering kinetic performance, solvent capacity, and energy demand. Working with higher solvent concentrations (2 M and 3 M) was found to be beneficial for both absorption and desorption in a DAC system due to their higher capacity (doubled to tripled), higher desorption rates and non-precipitating behavior. For the vacuum stripping process, operating at higher temperatures (70–90 °C) and vacuum pressures (21–81 $kPa_{(a)}$) enhanced the CO_2 removal flux. Notably, to harness the maximum enhanced effect of temperature and vacuum pressure, 0.23 mol/mol (~65 % loaded solvent) was considered the optimum resulting lean loading specification for 1 M GlyK. Interestingly, introducing a sweep gas stream to the vacuum system did not affect the CO_2 removal flux, which is attributed to the membrane PDMS dense layer. However, it remarkably escalated the water loss from the membrane module by up to three times. Hence, the vacuum mode without sweep gas was found to be more favorable. For simulation, a validated model was used to analyze the membrane thickness effect on DAC absorption–desorption performance. The model results highlighted the considerable improvement in CO_2 separation (over 100 %) when the dense layer thickness decreased from 55 μm to 1 μm which shows the effectiveness of hybrid technology of HFMCs in DAC operation. Hence, more long-term experimental trials of DAC using thinner membrane thicknesses needs to be completed. In general, the findings in this work

can start a new pathway for using HFMCs and green amino acid salt solutions in a sustainable DAC technology.

Declaration of competing interest

The authors declare that they have no known competing financial interests or personal relationships that could have appeared to influence the work reported in this paper.

Data availability

Data will be made available on request.

Appendix A. Supplementary data

Supplementary data to this article can be found online at https://doi.org/10.1016/j.cej.2023.147934.

References

[1] P.M. Cox, R.A. Betts, C.D. Jones, S.A. Spall, I.J. Totterdell, Acceleration of global warming due to carbon-cycle feedbacks in a coupled climate model, Nature 408 (6809) (2000) 184–187, https://doi.org/10.1038/35041539.

[2] EcoWatch, Atmospheric CO2 passes 420 PPM for first time ever, 2021. https://www.ecowatch.com/carbon-dioxide-exceeds-420-2651380906.html.

[3] IPCC, Global Warming of 1.5∘C, 2018. https://www.ipcc.ch/sr15/.

[4] E. Kriegler, N. Bauer, A. Popp, F. Humpenöder, M. Leimbach, J. Strefler, L. Baumstark, B.L. Bodirsky, J. Hilaire, D. Klein, I. Mouratiadou, I. Weindl, C. Bertram, J.-P. Dietrich, G. Luderer, M. Pehl, R. Pietzcker, F. Piontek, H. Lotze-Campen, A. Biewald, M. Bonsch, A. Giannousakis, U. Kreidenweis, C. Müller, S. Rolinski, A. Schultes, J. Schwanitz, M. Stevanovic, K. Calvin, J. Emmerling, S. Fujimori, O. Edenhofer, Fossil-fueled development (SSP5): An energy and resource intensive scenario for the 21st century, Glob. Environ. Chang. 42 (2017) 297–315, https://doi.org/10.1016/j.gloenvcha.2016.05.015.

[5] K.Z. Lackner, Hans-Joachim; Grimes, Patrick, Carbon Dioxide Extraction from Air: Is It An Option?, United States, 1999.

[6] F. Sabatino, A. Grimm, F. Gallucci, M. van Sint Annaland, G.J. Kramer, M. Gazzani, A comparative energy and costs assessment and optimization for direct air capture technologies, Joule 5(8) (2021) 2047-2076. 10.1016/j.joule.2021.05.023.

[7] N. McQueen, K.V. Gomes, C. McCormick, K. Blumanthal, M. Pisciotta, J. Wilcox, A review of direct air capture (DAC): scaling up commercial technologies and innovating for the future, Prog. Energy 3 (3) (2021), 032001, https://doi.org/10.1088/2516-1083/abf1ce.

[8] X. Zhu, W. Xie, J. Wu, Y. Miao, C. Xiang, C. Chen, B. Ge, Z. Gan, F. Yang, M. Zhang, D. O'Hare, J. Li, T. Ge, R. Wang, Recent advances in direct air capture by adsorption, Chem. Soc. Rev. 51 (15) (2022) 6574–6651, https://doi.org/10.1039/D1CS00970B.

[9] B. Dutcher, M. Fan, A.G. Russell, Amine-based CO2 capture technology development from the beginning of 2013—a review, ACS Appl. Mater. Interfaces 7 (4) (2015) 2137–2148, https://doi.org/10.1021/am507465f.

[10] S. Kim, H. Shi, J.Y. Lee, CO2 absorption mechanism in amine solvents and enhancement of CO2 capture capability in blended amine solvent, Int. J. Greenhouse Gas Control 45 (2016) 181–188, https://doi.org/10.1016/j.ijggc.2015.12.024.

[11] F.M. Brethomé, N.J. Williams, C.A. Seipp, M.K. Kidder, R. Custelcean, Direct air capture of CO2 via aqueous-phase absorption and crystalline-phase release using concentrated solar power, Nat. Energy 3 (7) (2018) 553–559, https://doi.org/10.1038/s41560-018-0150-z.

[12] R. Custelcean, N.J. Williams, K.A. Garrabrant, P. Agullo, F.M. Brethomé, H. J. Martin, M.K. Kidder, Direct air capture of CO2 with aqueous amino acids and solid bis-iminoguanidines (BIGs), Ind. Eng. Chem. Res. 58 (51) (2019) 23338–23346, https://doi.org/10.1021/acs.iecr.9b04800.

[13] A. Kiani, K. Jiang, P. Feron, Techno-economic assessment for CO2 capture from air using a conventional liquid-based absorption process, Front. Energy Res. 8 (2020), https://doi.org/10.3389/fenrg.2020.00092.

[14] W.M. Budzianowski, Explorative analysis of advanced solvent processes for energy efficient carbon dioxide capture by gas–liquid absorption, Int. J. Greenhouse Gas Control 49 (2016) 108–120, https://doi.org/10.1016/j.ijggc.2016.02.028.

[15] S. Laribi, L. Dubois, G. De Weireld, D. Thomas, Study of the post-combustion CO2 capture process by absorption-regeneration using amine solvents applied to cement plant flue gases with high CO2 contents, Int. J. Greenhouse Gas Control 90 (2019), 102799, https://doi.org/10.1016/j.ijggc.2019.102799.

[16] S. Lee, J. Kim, E. Lee, S. Hong, Improving the performance of membrane contactors for carbon dioxide stripping from water: Experimental and theoretical analysis, J. Membr. Sci. 654 (2022), 120552, https://doi.org/10.1016/j.memsci.2022.120552.

[17] J. Rivero, A. Lieber, C. Snodgrass, Z. Neal, M. Hildebrandt, W. Gamble, K. Hornbostel, Demonstration of direct ocean carbon capture using hollow fiber membrane contactors, Chem. Eng. J. 470 (2023), 143868, https://doi.org/10.1016/j.cej.2023.143868.

[18] J. Sun, P. Xu, D. Gong, X. Kong, K. Fu, X. Chen, M. Qiu, Y. Fan, Study on robust absorption performance of hydrophilic membrane contactor for direct air capture, Sep. Purif. Technol. 309 (2023), 122978, https://doi.org/10.1016/j.seppur.2022.122978.

[19] R. Castro-Muñoz, M. Zamidi Ahmad, M. Malankowska, J. Coronas, A new relevant membrane application: CO2 direct air capture (DAC), Chem. Eng. J. 446 (2022), 137047, https://doi.org/10.1016/j.cej.2022.137047.

[20] J.M. Vadillo, L. Gómez-Coma, A. Garea, A. Irabien, Hollow fiber membrane contactors in CO2 desorption: a review, Energy Fuel 35 (1) (2021) 111–136, https://doi.org/10.1021/acs.energyfuels.0c03427.

[21] T.J. Simons, P. Hield, S.J. Pas, A novel experimental apparatus for the study of low temperature regeneration CO2 capture solvents using hollow fibre membrane contactors, Int. J. Greenhouse Gas Control 78 (2018) 228–235, https://doi.org/10.1016/j.ijggc.2018.08.009.

[22] C.A. Scholes, S.E. Kentish, A. Qader, Membrane gas-solvent contactor pilot plant trials for post-combustion CO2 capture, Sep. Purif. Technol. 237 (2020), 116470, https://doi.org/10.1016/j.seppur.2019.116470.

[23] S. Kim, C.A. Scholes, D.E. Heath, S.E. Kentish, Gas-liquid membrane contactors for carbon dioxide separation: A review, Chem. Eng. J. 411 (2021), 128468, https://doi.org/10.1016/j.cej.2021.128468.

[24] H. Nieminen, L. Järvinen, V. Ruuskanen, A. Laari, T. Koiranen, J. Ahola, Insights into a membrane contactor based demonstration unit for CO2 capture, Sep. Purif. Technol. 231 (2020), 115951, https://doi.org/10.1016/j.seppur.2019.115951.

[25] D. Qi, K. Zhang, G. Tian, B. Jiang, Y. Huang, Stretchable electronics based on PDMS substrates, Adv. Mater. 33 (6) (2021) 2003155, https://doi.org/10.1002/adma.202003155.

[26] R. Ramezani, S. Mazinani, R. Di Felice, State-of-the-art of CO2 capture with amino acid salt solutions, 38(3) (2022) 273-299. https://doi.org/doi:10.1515/revce-2020-0012.

[27] L. Ansaloni, A. Hartono, M. Awais, H.K. Knuutila, L. Deng, CO2 capture using highly viscous amine blends in non-porous membrane contactors, Chem. Eng. J. 359 (2019) 1581–1591, https://doi.org/10.1016/j.cej.2018.11.014.

[28] M.S. Alivand, R.V. McQuillan, A. Momeni, A. Zavabeti, G.W. Stevens, K.A. Mumford, Facile Fabrication of Monodispersed Carbon Sphere: A Pathway Toward Energy-Efficient Direct Air Capture (DAC) Using Amino Acids, Small 2300150, doi: 10.1002/smll.202300150.

[29] R.V. McQuillan, A. Momeni, M.S. Alivand, G.W. Stevens, K.A. Mumford, Evaluation of Potassium Glycinate as a Green Solvent for Direct Air Capture and Modelling its Performance in Hollow Fiber Membrane Contactors, Chemical Engineering Journal, Under Review. (2023).

[30] M. Fang, Z. Wang, S. Yan, Q. Cen, Z. Luo, CO2 desorption from rich alkanolamine solution by using membrane vacuum regeneration technology, Int. J. Greenhouse Gas Control 9 (2012) 507–521, https://doi.org/10.1016/j.ijggc.2012.05.013.

[31] S. Khaisri, D. deMontigny, P. Tontiwachwuthikul, R. Jiraratananon, CO2 stripping from monoethanolamine using a membrane contactor, Journal of Membrane Science 376(1) (2011) 110-118. 10.1016/j.memsci.2011.04.005.

[32] S. Zhao, P.H.M. Feron, X. Chen, I. Boztepe, J. Zhang, N.R. Mirza, L. Kong, Gas flow enhanced mass transfer in vacuum membrane distillation, Desalination 552 (2023), 116434, https://doi.org/10.1016/j.desal.2023.116434.